CYCLIC PERFORMANCE OF REDUCED WEB SECTION (RWS) BEAM CONNECTIONS

Meysam Bayat [1], Konstantinos Daniel Tsavdaridis [2], AndresAlonso-Rodrıguez[3]

[1]*School of Science and Technology, City St George's, University of London, Northampton Square, London, EC1V 0HB, United Kingdom. meysam.bayat@city.ac.uk*

[2] *School of Science and Technology, City St George's, University of London, Northampton Square, London, EC1V 0HB, United Kingdom. konstantinos.tsavdaridis@city.ac.uk*

[3] *Faculty of Engineering, Universidad la Gran Colombia, Bogotá, 110231, Colombia. andalon@gmail.com*

SUMMARY:

This study provides an extensive analysis of Reduced Web Section (RWS) connections as a seismic retrofit strategy aimed at enhancing structural safety and sustainability in steel structures. RWS connections, which introduce perforations in the web of steel beams, offer a sustainable alternative to traditional Reduced Beam Section (RBS) connections by preserving flange integrity, minimising out-of-plane instability and slab connectivity. The research utilises 91 Finite Element Models validated against experimental data to assess the impact of web opening size and position on the cyclic performance of RWS connections subjected to the AISC 341 loading protocol. The findings demonstrate that with optimal design, RWS connections can achieve desirable failure modes, meeting AISC criteria for special moment frames with minimal strength degradation. The results show that specimens achieved ultimate drift demands over 4%, meeting AISC criteria for special moment frames with less than 20% strength degradation. This study highlights the potential of RWS connections, offering practical recommendations for their application in sustainable seismic retrofitting, structural rehabilitation, and improved structural safety.

KEYWORDS:

Seismic Retrofit, Reduced Web Section (RWS), Special Moment Frames, compliant RWS, Optimum Web Opening Size and Position.

1. INTRODUCTION

The construction of new steel structures exacerbates the climate crisis. The World Steel Association reports that the steel industry accounts for roughly 7-9% of global direct CO2 emissions [1]. Retrofitting existing steel buildings often represents a more sustainable and economical alternative to demolition and new construction [2]. Numerous studies have examined the effectiveness of different retrofitting methods in enhancing the strength and performance of existing buildings. Connections strengthening and beam weakening strategies have been extensively investigated as seismic retrofitting techniques to improve the ductility and performance of steel moment connections during earthquakes. Generally, these techniques are designed to pursue three primary targets.

1.1. OVERALL PERFORMANCE TARGETS FOR BEAM-TO-COLUMN CONNECTIONS

Eurocode 8 (BS/EN 1998-3) outlines three general recommendations for retrofitting design of structures for earthquake resistance [3]. i) The goal of the retrofit should be to shift the beam's plastic hinge away from the column face. ii) Beam-to-column connections can be retrofitted using weld replacement, a weakening strategy, or a strengthening strategy. iii) To ensure the development of plastic hinges in beams instead of columns, the column-to-beam moment ratio (CBMR) must exceed 1.3.

1.2. STRENGTHENING THE CONNECTIONS

Additions of haunches, cover plates, side plates, ribs, thickened webs, and widened flanges are typical examples of this technique. Several research papers have focused on connection-strengthening techniques and well-known guidelines such as FEMA 350, AISC, and prequalified connections to reduce earthquake risks. These connections are approved for use in special moment frame (SMF) and intermediate moment frame (IMF) systems within the limits of these provisions, with detailed design information available for practitioners. However, adding supplementary parts to the original beam or column section may impose a heavy load on the structure.

1.3. WEAKENING THE BEAMS

Generally, the aim is to locally reduce the beam's cross-sectional area at a certain distance from the connection to prevent brittle fractures in the joints and to ensure that inelasticity initiates within the beam in the designated protected zone. Reduced Beam Section (RBS) connections are the most common approach to weaken beam connections and protect joint welds from stress concentration. RBS connections have been extensively studied, and numerous studies have demonstrated their effectiveness, leading to their prequalification for practical design applications. Although cutting the beam flanges appears simple, this approach frequently becomes impractical for retrofit projects because of the demolition needed to reach the top flange, resulting in a cumbersome and inefficient process. Also, this approach introduces risks, including out-of-plane frame instability and lateral-torsional buckling in the beam, due to the reduced flange reducing the beam's torsional stiffness properties [4]. Another study showed that the RBS does not eliminate all inelastic strain demands at the beam flange weld [5].

An alternative connection involves RWS connections. The first proposal for the RWS technique was patented by Mark Amos Aschheim (January 11, 2000). It suggested the use of web voids to create dissipative zones that function as structural fuses, mitigating excessive stresses at connections and enhancing the seismic resilience of the structure [6]. This technique involves cutting the beam's web from the floor below, minimising disruption and eliminating the need for demolition. In addition, cost savings can be achieved by allowing mechanical equipment and utilities to pass through the web openings, decreasing the needed story height. Comprehensive studies have demonstrated that RWS connections can achieve high ductility and maintain stable hysteresis cycles, making them an efficient option for seismic retrofitting by both numerical simulations and laboratory testing [7] [8] [9] [10]. Furthermore, an experimental investigation contrasted RWS connections with RBS connections, demonstrating the superiority of RWS connections in terms of strength, stiffness, ductility, and lateral-torsional stability [4]. It should also be noted that reducing the flange area in the RBS connection can reduce frame stiffness and, subsequently, increase inter-storey drift demands. In contrast, this feature is expected to be smaller for RWS connections due to the smaller effect of reducing the web area on the moment of inertia of the cross-section [11]. On the other hand, the positive impact of single web openings on enhancing the rotational capacity of steel connections has been extensively studied [11] [12] [13] [14] [15] and [16].

Nevertheless, the design procedures concerning the upper and lower limits for geometric parameters remain to be established to the authors' best knowledge. Also, there are no established recommendations for the upper and lower limits of RWS connections' geometric parameters in the guidelines, although a few studies have proposed limited options for the geometric parameters [8] [17] [18]. In addition, despite ample evidence of the capabilities of RWS parameters for enabling stable inelastic action and leading to ductile fuses, criteria or recommendations for their application are still on their infancy. This is because the Recommended Seismic Design Criteria for New Steel Moment Frame Buildings (SAC Joint Venture), also known as FEMA 350, and the SAC Joint Venture has not reviewed the available data due to insufficient supporting information to verify compliance with the necessary prequalification criteria. As a result, although RWS connections were introduced briefly in Chapter

3.8.4 of FEMA-350 [19], they are not prequalified in the guidelines, and it is highlighted that "an understanding of the utility of this system for enduring seismic actions is developing".

To address this gap, this research aims to benchmark RWS connections by systematically evaluating the impact of cyclic drift demands, using Finite Element Analysis (FEA), following the weakening of the beam through perforations in its web and particularly, finding an effective range for a combination of depth of the web opening (d_o) and the distance from the face of the column to the centreline of the web opening (S), which are shown in Figure 1. To normalise these values, they are expressed as percentages of the beam depth (h). For example, if d_o=189mm and h=270mm, then d_o/h=189/270=0.7,

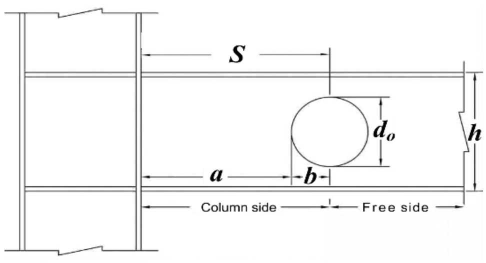

Figure 1. *RWS geometry*

or $(d_o/h)_{\%}$=70.

2. VALIDATION OF FE MODELS

This study employs a finite element model (FEM) in Abaqus, benchmarked against two experimental studies for parametric assessment. The first specimen is an RWS connection with a horizontal elliptical opening in the beam web (HE-RWS) in which IPE270 was used for the beam and IPB200 for the column. Section properties are equivalent to S235 in the European standard. More information can be found in [4]. The second specimen's name is DC-M, a welded unreinforced web connection to a box column (WUF-W). Further details of the connection and the experimental setup can be found in [20].

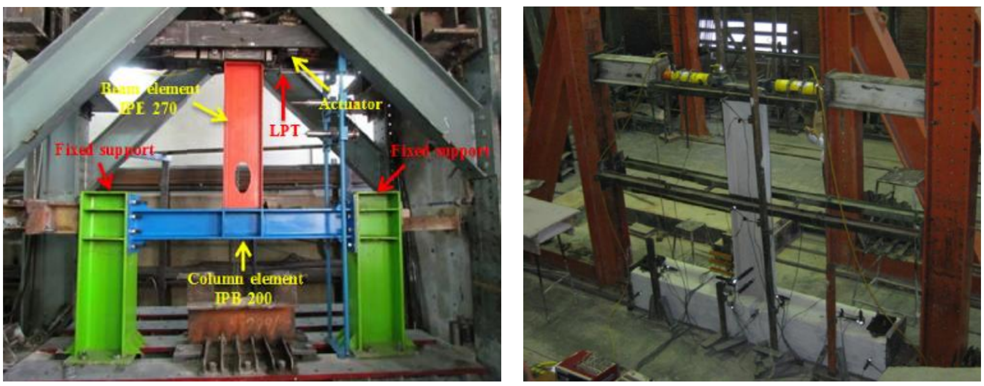

Figure 2. *HE-RWS (left), and DC-M (right) experiments*

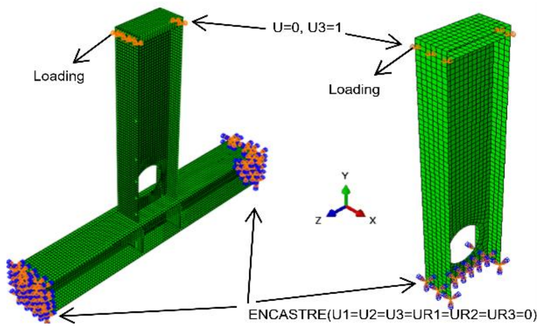

Figure 3. *Boundary conditions in the adopted FEMs: Left) scenario 1 (regular panel zone). Right) scenario 2 (represents a very strong panel zone)*

The primary FEM is shown in Figure 3 (left). After validating the FEM, the component method defined in Eurocode 3 is used to break down the connection into its constituent parts [21] assuming that the beam is affixed to a fixed support, Figure 3 (right). This approach isolates the impact of the web opening on the hysteretic behaviour of fully welded connections, providing a conservative bound for rotation capacities due to the scope of this study, which primarily focuses on the effect of web openings on the rotational capacity of beam-to-column connections. This method has been widely used in other studies [22] [23] [23] [24] [25] and [26]. Figure 3 (right) shows a beam modelled following earlier approaches. This ensures that changes in response are due to alterations in RWS geometry, providing clear insights into its behaviour under seismic cyclic loading and aiding in understanding the complex behaviour of RWS connections.

Cyclic loading is applied 35 mm from the top of the beam in both scenarios subjected to AISC 341 cyclic loading protocol [27]. After sensitivity studies, a quad-dominated element shape with a medial axis and a 15 mm mesh size algorithm were employed. At the same time, out-of-plane displacements are restricted by providing lateral support at boundaries. Also, tie constraints were used to model the welds.

The analysis presented in Figure 4 demonstrates an acceptable fit between results, confirming the efficacy of the current finite element model in predicting strength degradation due to local buckling in the plastic hinge region. The advantage of FEM of this study is that it employs a single Python script in Abaqus capable of accurately representing the moment-rotation hysteretic curves for two entirely different experiments with varying properties and geometries.

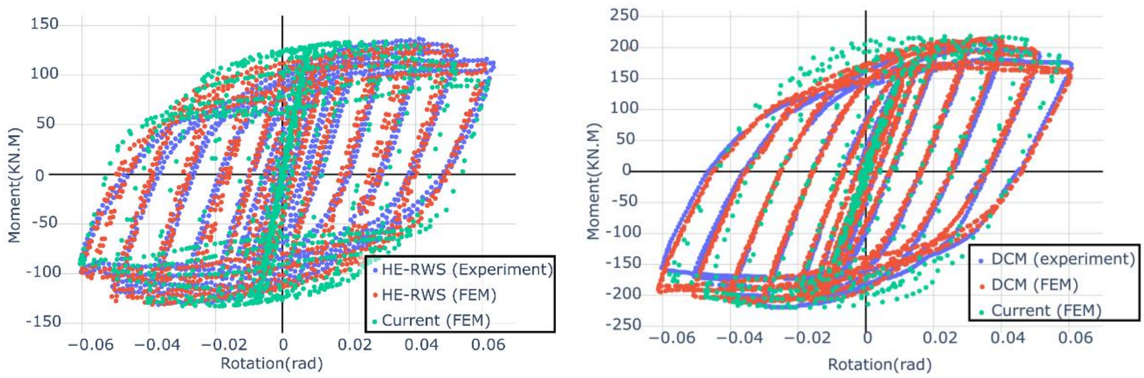

Figure 4. *Comparisons of the current FEM (green dots) with the experimental studies*

3. PARAMETRIC ANALYSIS WITH FIXED BEAM SUPPORT (SCENARIO 2)

The emphasis is on identifying combinations of (S) and (d_o) where yielding is confined to the protected zone surrounding the perforation while also adhering to capacity design principles. Focus is on four critical points: (i) the yield point *(My, θy)*, (ii) The peak moment *(Mm, θm)*, (iii) The ultimate strength and its ultimate rotation *(Mu, θu)*, and (iv) The $M_{0.04}$ is the observed moment strength at 0.04 rad rotation.

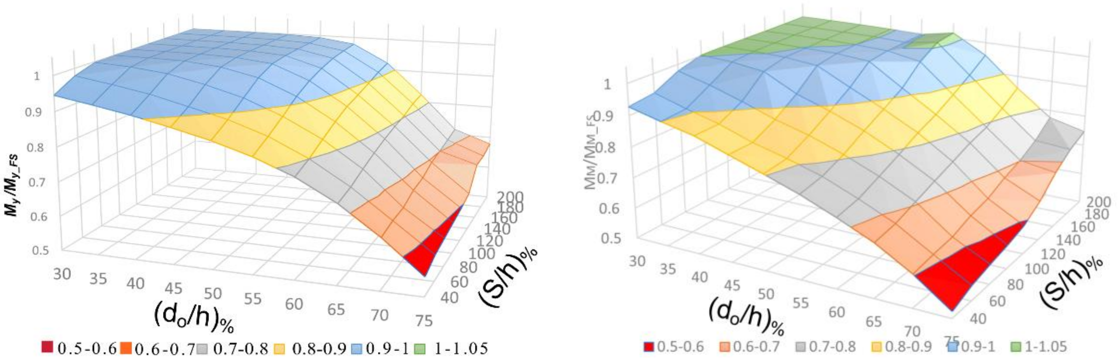

Figure 5. *The effect and the interaction of S and d_o on the yield moment and maximum moment strength (91 models normalised compared to that of the solid beam with Full section)*

This study conducts a comprehensive parametric analysis of 91 specimens featuring fixed beams. IPE270 beams with 10 web opening depths, d_o, ranging from 0.30h to 0.75h were analysed, considering nine S variations from 0.40h to 2h for each beam.

Specimens that could prevent inelastic action outside the protected zone are labelled NON-COMPLIANT RWS. Conversely, specimens that could prevent inelastic action outside the protected zone, meeting the AISC requirement of ‘the flexural strength cannot be less than 80% of *Mp* for a storey drift of 0.04 radian’, are labelled as COMPLIANT RWS. The criteria for categorising the connections involves reviewing Von Mises stresses, the PEEQ distribution, and principal strains to confirm that it deforms in a controlled, ductile manner and dissipates energy effectively. All combinations of d_o and S parameters that allow for compliance with capacity design principles are outlined in Figure 6.

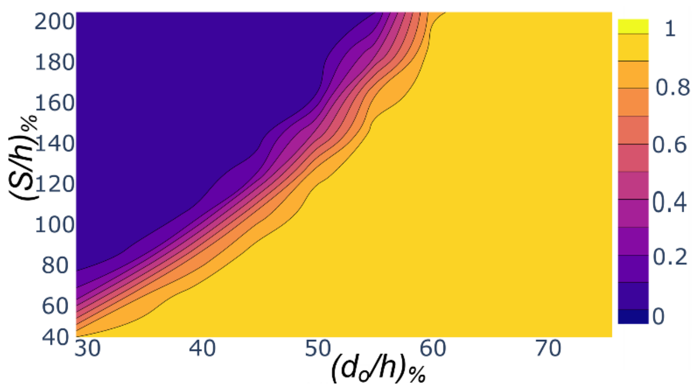

Figure 6. *Probability of yielding solely in the protected zone for combination S and d_o result in compliant RWS*

3.1. ROTATION CAPACITY AND STRENGTH DEGRADATION

The parametric assessments indicate that all specimens regarded in accordance with AISC 341 regulations exhibit highly ductile behaviour [27]. The peak moment consistently exceeds 80% of the maximum values for drifts below 0.04, thereby permitting the installation of connections within special moment frames following AISC 341 regulations [27]. Figure 7 illustrates that this applies to numerous web openings and spacings, thereby permitting flexibility.

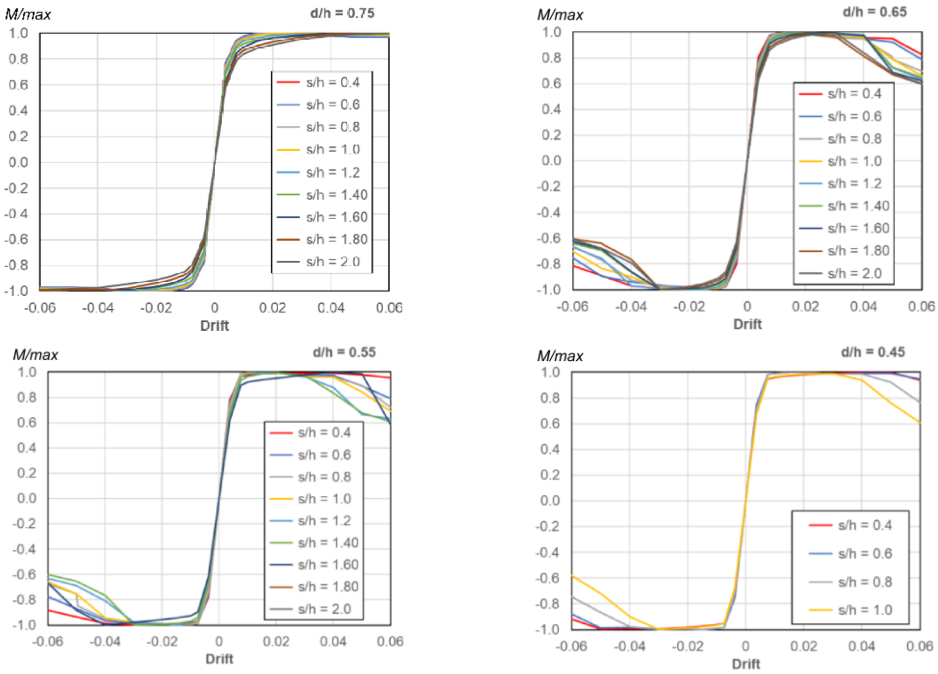

Figure 7. *Backbone curves for specimens with* $(d_o/h)_{\%}$ *= 0.75, 0.65, 0.55, 0.45*

4. CONCLUSIONS AND FURTHER STUDIES

This study confirms that Reduced Web Section (RWS) connections are an appealing option for seismic retrofitting, provided that the RWS geometric parameters are carefully selected within the recommended range. It was also observed that the S and d_o parameters are not independent variables; they should be chosen simultaneously due to their interaction effects on key design parameters to ensure an effective RWS connection. Additionally, it was determined that specific configurations of spacings from the column face and opening diameters resulted in plastic actions exclusively in the protected zone (Compliant RWSs). In addition, the parametric study demonstrates the ability of RWS connections to withstand 4% drift demands, following AISC 341-16 criteria for special moment frames [27], while exhibiting stable hysteresis cycles if the geometric parameters are selected appropriately. Similarly, the strength reduction beyond 4% drift demand was less than 20% in all cases assessed where yielding is inhibited outside the protected zone. This suggests that RWS connection is a ductile solution that can be deployed within special moment frames in accordance with AISC 341-16 [27].

On the other hand, beams with spacings to the centreline of the perforation from the column face less than one times the structural depth and openings less than half the structural depth are anticipated to develop moments exceeding 80% of the capacity of full-section beams. Furthermore, they will be capable of maintaining over 85% of the peak moment for deviations exceeding 4%.

This investigation aims to establish a framework for effectively utilising RWS connections as ductile solutions in the design of earthquake-resistant frames. It defines the detailed methodology that will be implemented while offering an overview of the potential desirable behaviour of RWS connections.

Residual stresses, imperfections, web slenderness, material grades, and other cross-sections are not considered in this study, as the objective was to establish a framework for defining the minimum conditions to evaluate the performance of RWS connection and outline the methodology. Once a design procedure has been established, systematic sensitivity analyses are necessary to ensure these factors are properly accounted for. This may require the evaluation of thousands of specimens, leading to a progression of this study.

5. REFERENCES

[1] World Steel Association, *Sustainability performance of the steel industry 2004-2022*. NA, 2023. [Online]. Available: https://worldsteel.org/steel-topics/sustainability/sustainability-indicators-2023-report/

[2] M. D. Alba-Rodríguez, A. Martínez-Rocamora, P. González-Vallejo, A. Ferreira-Sánchez, and M. Marrero, ‘Building rehabilitation versus demolition and new construction: Economic and environmental assessment’, *Environmental Impact Assessment Review*, vol. 66, pp. 115–126, Sep. 2017, doi: 10.1016/j.eiar.2017.06.002.

[3] Part 3 Eurocode 8, *BSI, BS EN 1998-3: design of structures for earthquake resistance-part 3: assessment and retrofitting of buildings*, 2005. doi: NA.

[4] M. Davarpanah, H. Ronagh, P. Memarzadeh, and F. Behnamfar, ‘Cyclic behavior of welded elliptical-shaped RWS moment frame’, *Journal of Constructional Steel Research*, vol. 175, p. 106319, Dec. 2020, doi: 10.1016/j.jcsr.2020.106319.

[5] ‘Behavior and Design of Radius Cut Reduced Beam Section Connections’. Accessed: Nov. 12, 2024. [Online]. Available: https://store.atcouncil.org/index.php?dispatch=products.view&product_id=132

[6] M. A. schheim, ‘MOMENT-RESISTANT STRUCTURE, SUSTAINER AND METHOD OF RESISTING EPISODIC LOADS’, 6,012,256, Jan. 2000 [Online]. Available: https://patents.google.com/patent/US6012256A/en

[7] K. D. Tsavdaridis, C. Pilbin, and C. K. Lau, ‘FE parametric study of RWS/WUF-B moment connections with elliptically-based beam web openings under monotonic and cyclic loading’, *Int J Steel Struct*, vol. 17, no. 2, pp. 677–694, Jun. 2017, doi: 10.1007/s13296-017-6023-7.

[8] Konstantinos Daniel Tsavdaridis and Theodore Papadopoulos, ‘Assessment of Beam-Column Connections Using Perforated Beams with Multiple Closely Spaced Web Openings’, *JCSR*, 2022, doi: 10.31224/2258.

[9] D. T. Naughton, K. D. Tsavdaridis, C. Maraveas, and A. Nicolaou, ‘Pushover Analysis of Steel Seismic Resistant Frames with Reduced Web Section and Reduced Beam Section Connections’, *Front. Built Environ.*, vol. 3, p. 59, Oct. 2017, doi: 10.3389/fbuil.2017.00059.

[10] K. D. Tsavdaridis, C. K. Lau, and A. Alonso-Rodríguez, ‘Experimental behaviour of non-seismical RWS connections with perforated beams under cyclic actions’, *Journal of Constructional Steel Research*, vol. 183, p. 106756, Aug. 2021, doi: 10.1016/j.jcsr.2021.106756.

[11] M. T. Kazemi and M. H. Asl, ‘Modeling of inelastic mixed hinge and its application in analysis of the frames with reduced beam section’, *Int J Steel Struct*, vol. 11, no. 1, pp. 51–63, Mar. 2011, doi: 10.1007/S13296-011-1005-7.

[12] A. A. Hedayat and M. Celikag, ‘Post-Northridge connection with modified beam end configuration to enhance strength and ductility’, *Journal of Constructional Steel Research*, vol. 65, no. 7, pp. 1413–1430, Jul. 2009, doi: 10.1016/j.jcsr.2009.03.007.

[13] Q. Yang, B. Li, and N. Yang, ‘Aseismic behaviors of steel moment resisting frames with opening in beam web’, *Journal of Constructional Steel Research*, vol. 65, no. 6, pp. 1323–1336, Jun. 2009, doi: 10.1016/j.jcsr.2009.01.007.

[14] G. S. Prinz and P. W. Richards, 'Eccentrically braced frame links with reduced web sections', *Journal of Constructional Steel Research*, vol. 65, no. 10–11, pp. 1971–1978, Oct. 2009, doi: 10.1016/j.jcsr.2009.04.017.

[15] K. D. Tsavdaridis, 'Strengthening Techniques: Code-Deficient Steel Buildings', in *Encyclopedia of Earthquake Engineering*, M. Beer, I. A. Kougioumtzoglou, E. Patelli, and I. S.-K. Au, Eds., Berlin, Heidelberg: Springer Berlin Heidelberg, 2014, pp. 1–26. doi: 10.1007/978-3-642-36197-5_207-1.

[16] V. Akrami and S. Erfani, 'Review and Assessment of Design Methodologies for Perforated Steel Beams', *J. Struct. Eng.*, vol. 142, no. 2, p. 04015148, Feb. 2016, doi: 10.1061/(ASCE)ST.1943-541X.0001421.

[17] K. Boushehri, K. D. Tsavdaridis, and G. Cai, 'Seismic behaviour of RWS moment connections to deep columns with European sections', *Journal of Constructional Steel Research*, vol. 161, pp. 416–435, Oct. 2019, doi: 10.1016/j.jcsr.2019.07.009.

[18] M. Davarpanah, H. Ronagh, P. Memarzadeh, and F. Behnamfar, 'Cyclic behaviour of elliptical-shaped reduced web section connection', *Structures*, vol. 24, pp. 955–973, Apr. 2020, doi: 10.1016/j.istruc.2020.02.016.

[19] S. FEMA 350, *Seismic Design Criteria for New Steel Moment Frame Buildings*, NA., NA vols. in NA, no. NA. NA: NA, 2001. [Online]. Available: https://ascelibrary.org/doi/abs/10.1061/40558%282001%29149

[20] Z. Saneei Nia, M. Ghassemieh, and A. Mazroi, 'WUF-W connection performance to box column subjected to uniaxial and biaxial loading', *Journal of Constructional Steel Research*, vol. 88, pp. 90–108, Sep. 2013, doi: 10.1016/j.jcsr.2013.04.008.

[21] *Eurocode 3: Design of Steel Structures–Part 1–8: Design of Joints*, 2005. doi: NA.

[22] S. M. Mojtabaei, J. Becque, and I. Hajirasouliha, 'Behavior and Design of Cold-Formed Steel Bolted Connections Subjected to Combined Actions', *J. Struct. Eng.*, vol. 147, no. 4, p. 04021013, Apr. 2021, doi: 10.1061/(ASCE)ST.1943-541X.0002966.

[23] D. T. Phan, S. M. Mojtabaei, I. Hajirasouliha, T. L. Lau, and J. B. P. Lim, 'Design and Optimization of Cold-Formed Steel Sections in Bolted Moment Connections Considering Bimoment', *J. Struct. Eng.*, vol. 146, no. 8, p. 04020153, Aug. 2020, doi: 10.1061/(ASCE)ST.1943-541X.0002715.

[24] T. A. Horton, I. Hajirasouliha, B. Davison, and Z. Ozdemir, 'More efficient design of reduced beam sections (RBS) for maximum seismic performance', *Journal of Constructional Steel Research*, vol. 183, p. 106728, Aug. 2021, doi: 10.1016/j.jcsr.2021.106728.

[25] T. A. Horton, I. Hajirasouliha, B. Davison, and Z. Ozdemir, 'Accurate prediction of cyclic hysteresis behaviour of RBS connections using Deep Learning Neural Networks', *Engineering Structures*, vol. 247, p. 113156, Nov. 2021, doi: 10.1016/j.engstruct.2021.113156.

[26] T. A. Horton, I. Hajirasouliha, B. Davison, Z. Ozdemir, and I. Abuzayed, 'Development of more accurate cyclic hysteretic models to represent RBS connections', *Engineering Structures*, vol. 245, p. 112899, Oct. 2021, doi: 10.1016/j.engstruct.2021.112899.

[27] AISC 341-16, 'Seismic Provisions for Structural Steel Buildings', *American Institute of Steel Construction*, Jan. 2016, doi: NA.

Appendix A

Table A1. *Summary table of 90 FEMs with fixed beams (θu and Mu of non-deteriorating models in this table are ignored due to their unclear cyclic deterioration)*

Model	Area(mm^2)	$(do/h)_{\%}$	$(S/h)_{\%}$	My(FE)	My(AISC)	θm	Mm	−θm	−Mm	θu	Mu	Ediss
FS	0	0	0	131.9	128.3	4	146.2	-4	-145.5	-	-	18.4
C-1	5150	30	40	124.7	125.4	4	135.6	-4	-134.6	-	-	17.8
C-2	7010	35	40	122.4	124.4	4	131.7	-4	-130.6	-	-	17.5
C-3	9156	40	40	119.7	123.2	5	128.1	-5	-127.2	-	-	17.2

C-4	11588	45	40	116.6	121.8	5	122.7	-3	-122.3	-	-	16.6
C-5	14306	50	40	113.1	120.3	4	117.4	-3	-118.6	-	-	16.1
C-6	17311	55	40	108.8	118.6	2	111.8	-3	-112.6	-	-	15.1
C-7	20601	60	40	103.1	116.8	2	105.2	-1.5	-105.0	-	-	14.0
C-8	24178	65	40	95.3	114.8	1.5	97.9	-1.5	-98.0	-	-	12.8
C-9	28040	70	40	85.1	112.6	1.5	88.2	-1.5	-87.9	-	-	11.9
C-10	32189	75	40	73.1	110.3	1.5	76.2	-1.5	-76.0	-	-	10.7
C-11	5150	30	60	129.1	125.4	6	137.2	-5	-135.6	-	-	18.6
C-12	7010	35	60	126.8	124.4	6	132.5	-3	-131.2	-	-	17.9
C-13	9156	40	60	124.3	123.2	5	128.3	-3	-127.5	-	-	17.3
C-14	11588	45	60	120.8	121.8	2	122.8	-3	-122.6	-	-	16.5
C-15	14306	50	60	117.2	120.3	1.5	118.6	-1.5	-118.8	-	-	15.5
C-16	17311	55	60	112.4	118.6	1.5	113.8	-1.5	-113.6	5.9	91	14.5
C-17	20601	60	60	105.6	116.8	1.5	107.1	-1.5	-106.9	-	-	13.7
C-18	24178	65	60	96.8	114.8	1.5	99.6	-1.5	-99.3	5.8	79.7	12.4
C-19	28040	70	60	86.3	112.6	1.5	89.7	-1.5	-89.5	-	-	11.6
C-20	32189	75	60	75.6	110.3	1.5	80.0	-1.5	-79.8	-	-	10.7
C-21	5150	30	80	131.6	125.4	4	143.1	-4	-142.2	-	-	18.8
C-22	7010	35	80	130.8	124.4	4	138.9	-4	-137.9	-	-	18.1
C-23	9156	40	80	129.1	123.2	4	133.9	-3	-133.7	5.7	107.1	16.7
C-24	11588	45	80	126.0	121.8	2	128.3	-1.5	-128.1	5.7	102.6	16.0
C-25	14306	50	80	122.1	120.3	1.5	123.9	-1.5	-123.8	5.7	99.1	15.3
C-26	17311	55	80	116.3	118.6	1.5	118.1	-1.5	-117.7	5.5	94.4	14.2
C-27	20601	60	80	109.0	116.8	1.5	111.3	-1.5	-111.1	5.6	89	13.5
C-28	24178	65	80	99.3	114.8	1.5	103.1	-1.5	-103.0	4.9	82.5	12.2
C-29	28040	70	80	86.4	112.6	1.5	90.8	-1.5	-90.8	-	-	11.7
C-30	32189	75	80	76.7	110.3	2	82.2	-3	-82.1	-	-	10.8
C-31	5150	30	100	131.9	125.4	4	146.4	-4	-145.6	-	-	18.8
C-32	7010	35	100	131.8	124.4	4	145.5	-4	-144.8	-	-	18.7
C-33	9156	40	100	131.4	123.2	4	143.4	-4	-142.4	-	-	18.4
C-34	11588	45	100	130.0	121.8	3	135.4	-3	-136.5	4.8	108.3	15.2
C-35	14306	50	100	126.8	120.3	2	130.0	-1.5	-130.0	4.7	104	14.6
C-36	17311	55	100	120.7	118.6	1.5	123.7	-1.5	-123.5	5.2	99	14.3
C-37	20601	60	100	112.2	116.8	1.5	115.7	-1.5	-115.9	4.8	92.6	13.2
C-38	24178	65	100	101.5	114.8	1.5	106.6	-1.5	-106.6	4.9	85.3	12.2
C-39	28040	70	100	88.7	112.6	2	94.0	-2	-93.8	5.8	75.2	11.7
C-40	32189	75	100	77.7	110.3	2	84.0	-3	-84.4	-	-	11.0
C-41	5150	30	120	131.9	125.4	4	146.5	-4	-145.5	-	-	18.8
C-42	7010	35	120	131.8	124.4	4	146.4	-4	-144.1	-	-	18.7
C-43	9156	40	120	131.7	123.2	4	145.9	-4	-145.5	-	-	18.7
C-44	11588	45	120	131.2	121.8	4	144.4	-4	-144.1	-	-	18.7
C-45	14306	50	120	129.6	120.3	3	136.5	-3	-137.7	-	-	18.7
C-46	17311	55	120	123.9	118.6	1.5	128.8	-1.5	-128.6	4.3	103.1	13.6
C-47	20601	60	120	114.9	116.8	1.5	120.5	-1.5	-120.7	4.5	96.4	12.7
C-48	24178	65	120	103.4	114.8	1.5	109.9	-1.5	-109.9	4.6	87.9	12.3
C-49	28040	70	120	89.3	112.6	2	95.8	-3	-95.8	5.7	76.6	11.7
C-50	32189	75	120	78.7	110.3	4	86.5	-3	-87.1	-	-	11.2
C-51	5150	30	140	131.9	125.4	4	146.5	-4	-146.0	-	-	18.8
C-52	7010	35	140	131.8	124.4	4	146.5	-4	-145.4	-	-	18.7
C-53	9156	40	140	131.8	123.2	4	146.2	-3	-141.7	-	-	18.6
C-54	11588	45	140	131.4	121.8	4	145.9	-4	-144.2	-	-	18.5
C-55	14306	50	140	130.4	120.3	4	144.5	-4	-144.5	-	-	18.6
C-56	17311	55	140	126.1	118.6	2	134.2	-3	-134.7	4.2	107.3	13.7
C-57	20601	60	140	116.5	116.8	1.5	124.2	-1.5	-124.0	4.6	99.3	13.0
C-58	24178	65	140	104.8	114.8	2	113.4	-3	-113.5	4.7	90.7	12.3
C-59	28040	70	140	91.5	112.6	4	99.7	-3	-100.1	5.4	79.8	11.7
C-60	32189	75	140	80.3	110.3	6	90.4	-6	-90.9	-	-	11.6
C-61	5150	30	160	131.9	125.4	4	146.4	-4	-146.2	-	-	18.8
C-62	7010	35	160	131.8	124.4	4	146.6	-4	-146.2	-	-	18.8
C-63	9156	40	160	131.7	123.2	4	146.5	-4	-145.7	-	-	18.7
C-64	11588	45	160	131.5	121.8	4	146.2	-4	-146.0	-	-	18.7
C-65	14306	50	160	130.7	120.3	4	145.5	-4	-145.3	-	-	18.7
C-66	17311	55	160	127.7	118.6	4	142.6	-4	-142.5	5.4	114	16.2
C-67	20601	60	160	118.3	116.8	2	128.9	-2	-128.1	3.9	103.1	12.7
C-68	24178	65	160	105.9	114.8	2	115.8	-3	-116.6	4.6	92.6	12.3
C-69	28040	70	160	92.4	112.6	4	102.5	-3	-102.5	5.2	82	11.8
C-70	32189	75	160	88.0	110.3	6	104.1	-6	-103.2	-	-	12.6
C-71	5150	30	180	131.9	125.4	4	146.4	-4	-145.6	-	-	18.7
C-72	7010	35	180	131.8	124.4	4	146.5	-4	-146.1	-	-	18.8
C-73	9156	40	180	131.7	123.2	4	146.5	-4	-145.8	-	-	18.7
C-74	11588	45	180	131.5	121.8	4	146.3	-4	-146.1	-	-	18.8
C-75	14306	50	180	130.9	120.3	4	145.7	-4	-145.6	-	-	18.6
C-76	17311	55	180	128.4	118.6	5	147.9	-4	-143.9	-	-	18.7
C-77	20601	60	180	120.2	116.8	3	134.1	-3	-134.9	4.4	107.2	13.3
C-78	24178	65	180	107.8	114.8	2	120.2	-3	-122.2	4.1	96.1	12.2
C-79	28040	70	180	93.5	112.6	4	106.9	-3	-105.7	5.4	85.5	12.2
C-80	32189	75	180	87.9	110.3	6	106.9	-6	-106.5	-	-	12.7

C-81	5150	30	200	131.9	125.4	4	146.5	-4	-146.0	-	-	18.8
C-82	7010	35	200	131.8	124.4	4	146.6	-4	-146.3	-	-	18.8
C-83	9156	40	200	131.8	123.2	4	146.5	-4	-146.2	-	-	18.8
C-84	11588	45	200	131.6	121.8	4	146.3	-4	-145.9	-	-	18.7
C-85	14306	50	200	131.0	120.3	4	145.8	-4	-145.7	-	-	18.6
C-86	17311	55	200	129.0	118.6	5	148.7	-5	-147.2	-	-	18.7
C-87	20601	60	200	121.5	116.8	4	139.8	-4	-139.5	4.6	111.8	14.5
C-88	24178	65	200	108.7	114.8	3	125.6	-3	-126.3	4.2	100.5	12.5
C-89	28040	70	200	94.6	112.6	4	110.4	-4	-109.3	5	88.3	12.2
C-90	32189	75	200	89.5	110.3	6	113.5	-6	-111.8	-	-	13.1

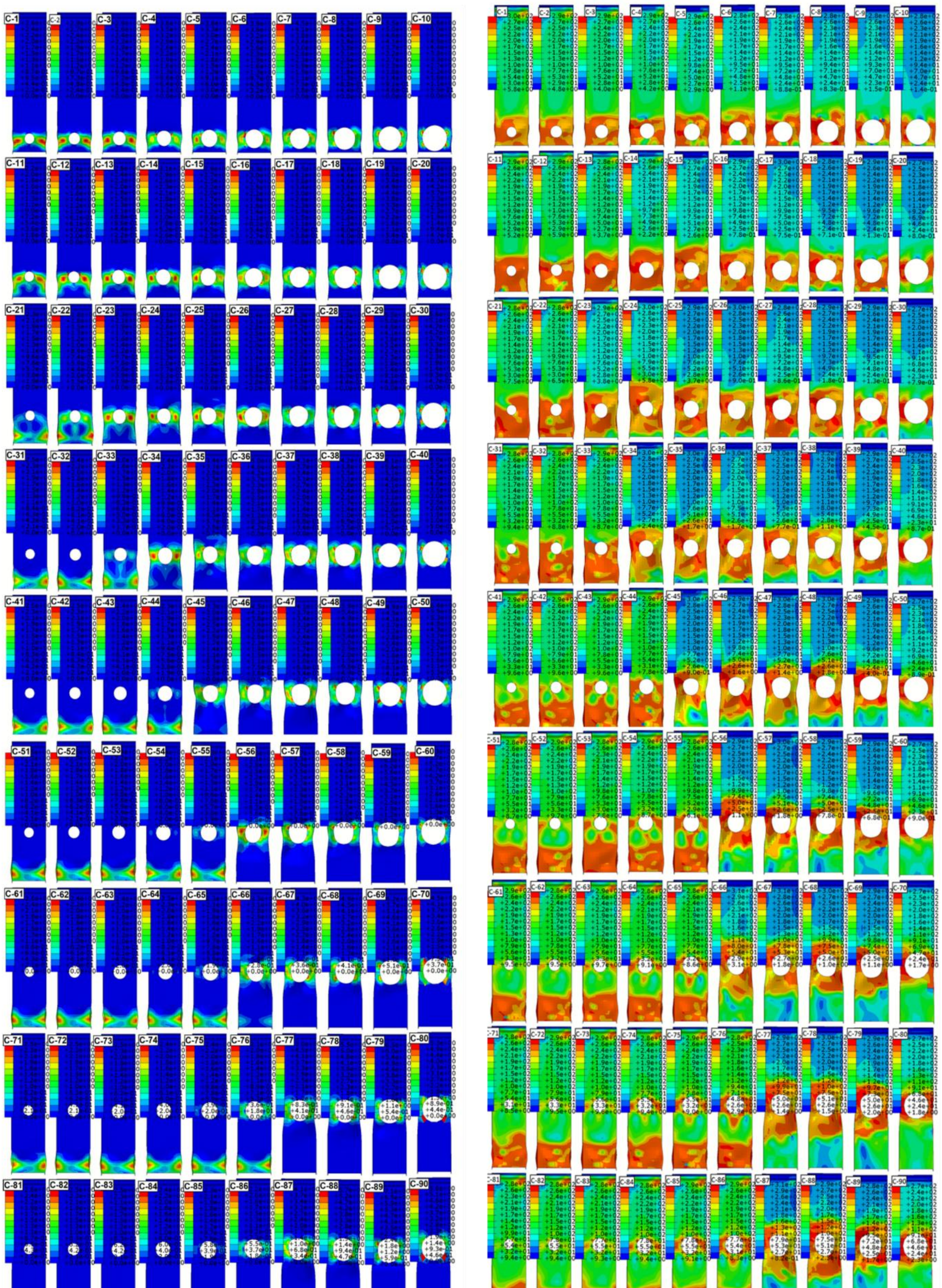

Figure A1. *PEEQ distributions, and Von Mises contour plots, with different (S and d_o) (90combinations)*